Prokaryotic communities across oceanic depths produce stable dissolved organic nitrogen

Richard LaBrie[1,#,*], Nagissa Mahmoudi[2], Luc Tremblay[3], Jennifer Cherrier[4], Jean-Éric Tremblay[5] and Roxane Maranger[1]

[1]Département des sciences biologiques and Groupe de recherche interuniversitaire en limnologie et environnement aquatique (GRIL), Université de Montréal, Pavillon MIL C. P. 6128, succ. Centre-ville, Montréal, QC, Canada, H3C 3J7

[2]Department of Earth & Planetary Sciences, McGill University, 3450 rue University, Montréal, Québec, Canada, H3A 2A7

[3]Département de chimie et biochimie, Université de Moncton, 18, avenue Antonine-Maillet, Moncton, NB, Canada, E1A 3E9

[4]Department of Earth and Environmental Sciences, Brooklyn College-The City University of New York, 2900 Bedford Avenue, Brooklyn, NY 11210, USA

[5]Québec-Océan and Takuvik, Département de biologie, Université Laval, 1045 avenue de la Médecine, Québec, Canada, G1V 0A6

[#]Current affiliation: Department of Earth & Planetary Sciences, McGill University, 3450 rue University, Montréal, Québec, Canada, H3A 2A7

*Corresponding author

Email: Richard.labrie90@gmail.com

ORCID

RL 0000-0003-1681-4888

NM 0000-0001-9118-4180

LT 0000-0002-7515-7788

JC 0000-0003-4687-7783

JET 0000-0003-0319-5723

RM 0000-0002-2509-4678

Keywords

Microbial nitrogen pump, nitrogen cycling, carbon cycling, biogeochemistry, Labrador Sea

Scientific significance statement

Dissolved organic nitrogen (DON) is one of the largest and least understood global N reservoirs. Yet, DON is critical for the growth of microorganisms but a significant amount of it persists in water, even in nutrient-poor regions such as gyres and the deep ocean where its consumption would be most beneficial. Different mechanisms could produce long-lived DON, including through microbial production and reprocessing of organic matter, a microbial N pump. However, it is not clear whether long-lived DON is produced equally across all water depths. In this study, we provide evidence that microbes from all oceanic depths can produce this stable material, but this production is likely more important in the surface ocean where microbes encounter more bioavailable organic matter.

ABSTRACT

It has been hypothesized that refractory dissolved organic nitrogen (RDON) may originate from successive microbial reprocessing of labile compounds, a process termed microbial nitrogen pump (MNP). However, it is still unknown whether microbial communities from different oceanic depths are equally efficient in producing RDON. We tested the MNP by mixing surface dissolved organic matter (DOM) with prokaryotic communities from the surface, meso- and bathypelagic regions of the Labrador Sea, and tracked changes in DON concentration and composition over time in bottle incubations. Prokaryotic communities from all depths were equally proficient at producing RDON as evidenced by increased fluorescent DOM associated with recalcitrant molecules, consistent degradation patterns based on amino acid yields and composition, and similar molecular composition. As RDON production depends on the reprocessing of labile and semi-labile substrate, we

hypothesized that the MNP is more important in the surface ocean where fresher DOM is more available for prokaryotic growth.

INTRODUCTION

Dissolved organic nitrogen (DON) is critical for the growth and productivity of marine microorganisms and represents the largest reservoir of fixed N in the surface ocean (Aluwihare and Meador 2008). Similar to the dissolved organic carbon (DOC) pool, a large portion of DON is refractory (McCarthy et al. 1997). Many explanations have been proposed for the origin and formation of refractory DOC (RDOC), including photochemistry (Benner and Biddanda 1998), continental runoff (Lønborg and Álvarez-Salgado 2012), hydrothermal sources (Yamashita et al. 2023), and bacterial production from labile substrates (Ogawa et al. 2001). The latter is referred to as the "microbial carbon pump" (MCP, Jiao et al. 2010) and has been demonstrated in laboratory experiments where marine prokaryotes produced RDOC from simple and more complex organic compounds (Ogawa et al. 2001; Lechtenfeld et al. 2014; Benner and Amon 2015). It has been hypothesized that refractory DON (RDON) may originate similarly from a "microbial nitrogen pump" (MNP) where microbial reprocessing of labile DON produces more recalcitrant dissolved compounds (Yamaguchi and McCarthy 2018). Despite the importance of DON, studies on the MNP are rare, and most of the evidence are derived from amino acid (AA) yields and distribution (Yamaguchi and McCarthy 2018; Broek et al. 2019). Thus, how the MNP may shape a N sequestration remains underexplored.

The chemical composition of the DON pool appears simpler than DOC (McCarthy et al. 1997; Sipler and Bronk 2015). Throughout oceanic depths, almost all the N in high molecular weight (>1000 dalton) dissolved organic matter (DOM) is in amide groups (McCarthy et al. 1997). The low molecular weight (LMW) fraction also appears to be chemically similar across oceanic depths, consisting of N-heterocycles (i.e., aromatic rings composed with at least one N atom) and amide groups (Broek et al. 2023). Despite the apparent compositional simplicity and consistency of DON, the depths at which these molecules are mainly produced remain to be elucidated. Based on δ^{15}N-AA profiles, it has been recently hypothesized that RDON production may be mostly constrained to the surface ocean and mixed into the deep ocean (Ianiri and McCarthy 2023). However, deep prokaryotic communities were comparatively more efficient at producing stable DOC in the MCP (LaBrie et al. 2022). If similar communities also produce RDON, then the MNP could be most effective in the deep ocean.

Given the range of physical and biological factors that influence the microbial production and cycling of DON, characterizing these processes in natural environments remains a challenge (Sipler and Bronk 2015). Experimental bottle incubations enable this type of investigation, and we recently used this approach to characterize how prokaryotes from different ocean depths, from the deep winter convection region of the Labrador Sea (Yashayaev and Loder 2017), transform surface DOC (LaBrie et al. 2022). The production of RDON and RDOC are likely intertwined, as C and N are fundamental elements of DOM and their cycles are closely linked (Sipler and Bronk 2015). Here, we used the aforementioned Labrador Sea incubation experiments to address two key questions related

to RDON production: 1) did microbial DON increase following surface DOM transformation? 2) can deep prokaryotic communities produce and sequester DON more efficiently than surface communities? Specifically, we looked at changes in bulk DON concentration and different molecular markers to assess production and transformation. Composition was assessed by fluorescent DOM (FDOM), giving a semiquantitative description of broad functional groups (Murphy et al. 2014), AA analysis, identifying main DON compounds (McCarthy et al. 1997), and Fourier transform ion cyclotron resonance mass spectrometry (FT-ICR-MS) for a qualitative characterization of LMW DON (Hawkes et al. 2020), thus providing a holistic view of DON dynamics.

MATERIALS AND METHODS

Site and bottle incubations

Samples from the surface (20 m), mesopelagic (540 m) and bathypelagic (1500 m) were taken near the central station (57.59°N, 51.57°W, Fig. S1) of the Atlantic Repeat Hydrography Line 7 West in the Labrador Sea on May 14, 2016. Seawater for bottle incubations was collected and meshed (53 µm) into acid-washed high-density polyethylene carboys and transported to the ship-based laboratory for processing. Replicate treatment bottles were prepared by mixing 8 L of filtered (3 µm polycarbonate and 0.2 µm polyethersulfone filters using a peristaltic pump) surface water (medium) with 2 L (inoculum) of water collected from the surface, mesopelagic or bathypelagic. Meso- and bathypelagic treatments are referred to as “deep” when discussed together. Incubations were carried out in 11 L acid and base washed glass bottles with silicone stoppers for 18

months (LaBrie et al. 2022). Abiotic conditions (no light and temperature at 4°C) were constant during the entire experiment.

Treatment bottles were sampled multiple times during the first three months, and at six, nine and 18 months, for a total of 11 sampling events. At each time point, water was poured into an acid washed, pre-conditioned glass bottle to avoid contamination. Subsamples were collected for various chemical analyses (DOC, DON, FDOM, AA, FT-ICR-MS) described in LaBrie et al. (2022).

DON quantification

DON was calculated as the difference between total dissolved nitrogen (TDN) and dissolved inorganic nitrogen (DIN). DIN and TDN were measured on days 0, 4, 7, 16, 21, 31, 62, 92, 183 and 274. TDN samples were acidified at pH < 2 using concentrated HCl (12 M, Fisher Scientific ACSPlus) and stored in pre-combusted (450 °C for 5 h) amber glass vials at 4°C. Since incubation waters were prefiltered, TDN samples were not filtered again but particulate organic nitrogen is considered negligible. TDN was measured on a Shimadzu TOC-L/TN-TMNL analyzer with a detection limit of 0.08 µmol N L^{-1} at Brooklyn College, and validated against deep seawater reference material (Hansell 2005).

Samples for DIN (nitrate + nitrite + ammonium) were filtered through 0.7 µm pre-combusted glass fiber filters, where nitrate and nitrite were stored frozen in 15 mL polyethylene tubes until analysis using a colorimetric method on a Bran and Luebbe Autoanalyzer II (SEAL Analytical, WI, USA) at Université Laval. Ammonium was

145 measured immediately using derivatization with o-phthaldialdehyde (OPA) and
146 fluorometric detection on a TD-700 fluorimeter (Turner Designs, CA, USA) (Holmes et al.
147 1999). Detection limits were 0.04 µmol L^{-1} for nitrite, 0.01 µmol L^{-1} for nitrate, and
148 0.02 µmol L^{-1} for ammonium.
149
150 **Broad DON characterization using optical properties**
151 FDOM concentration was monitored over time to assess the cycling of labile and
152 recalcitrant DOM using a bulk approach using excitation-emission matrices coupled with
153 parallel factor (PARAFAC) analysis (see LaBrie et al. 2022). The PARAFAC model
154 included four different peaks (Fig. S2), three of which may be related to DON. Peaks will
155 be referred to as $F_{\lambda em}X$, where X is the emission wavelength at maximum intensity (LaBrie
156 et al. 2020), which is related to compound aromaticity (Romera-Castillo et al. 2011). Peaks
157 $F_{\lambda em}302$ and $F_{\lambda em}340$ are considered two protein-like N-containing compounds that include
158 tyrosine and tryptophan, respectively, and $F_{\lambda em}392$ has recently been associated with the
159 recalcitrant compound dityrosine (Coble 1996; Paerl et al. 2020). FDOM was measured on
160 days 0, 4, 16, 31, 92, 183 and 547 and values are reported in Raman units to compare with
161 other studies.
162
163 **Amino acid quantification**
164 The concentration of 23 AA were monitored in unfiltered water samples as an indicator of
165 labile DON (Amon et al. 2001) and to calculate markers of DOM degradation state (see
166 below). AA peptide bonds (e.g. in proteins and peptides) were hydrolyzed (HCl 6 M,
167 110 °C for 20 h). Free and hydrolyzed AA were then derivatized into fluorescent

complexes that were separated by reversed-phase high precision liquid chromatography (HPLC) and detected by a fluorescent detector at Université de Moncton as in Escoubeyrou and Tremblay (2014), with certain modifications (Hébert and Tremblay 2017). Quantification was done using external calibration with AA standard mixtures (see Supporting information, SI).

Total hydrolysable AA (THAA) represent the sum of all free AA and hydrolysable combined AA. Using the molar concentration of individual AA, we calculated the Dauwe index (DI) and the fraction of N as THAA ($\%N_{THAA}$). These two markers decrease with DOM degradation (Cowie and Hedges 1994; Dauwe et al. 1999; Tremblay and Benner 2009) although $\%N_{THAA}$ is more sensitive to early DOM transformation (Davis et al. 2009; Bourgoin and Tremblay 2010). More details are provided in the SI. AA were quantified at the same time points as DON concentration, except at days 61 and 274 when no samples were taken.

DON chemical characterization via FT-ICR-MS

To investigate how prokaryotic communities altered the DON pool at a molecular level, we characterized DOM using FT-ICR-MS. Solid-phase extracted (SPE) DOM was recovered using styrene-divinylbenzene cartridges (Bond Elut PPL cartridges, Agilent) using standard extraction procedures (Dittmar et al. 2008). SPE-DOM was characterized using a 9.4 tesla FT-ICR-MS with electrospray ionization in negative mode at the National High Magnetic Field Laboratory in Tallahassee, USA (see LaBrie et al. 2022 for more

details). We focused on N-containing molecular formulae (N-MF) changes between samples collected at day 0 and after 92 days of microbial transformations.

Data analyses were performed on R Studio (R Core Team 2022).

RESULTS

Early DON production

Changes in bulk DON concentrations examined over nine months (Fig. 1) revealed similar temporal patterns between surface and bathypelagic treatments, with a DON concentration increase from day 0 to 31 or 62, respectively, followed by stabilization. DON concentration in the mesopelagic treatment also increased from day 0 to day 31, but then decreased before stabilization. In the later stages of incubations, DON concentrations remained relatively constant at 5.34 ± 0.85 µmol N L^{-1} (mean ± sd) across treatments. This accumulation of DON indicates a transformation of inorganic N into organic forms, a phenomenon known as N-immobilization (Tremblay and Benner 2006; Bourgoin and Tremblay 2010) that was likely caused by a N-poor DOM source (Fig. S3). Indeed, the dominant phytoplankton species at the time of sampling was *Prorocentrum sp.* (Péquin et al. 2022), a dinoflagellate known to exude transparent exopolymers, a class of compound rich in polysaccharides (Larsson et al. 2022; Tillmann et al. 2023).

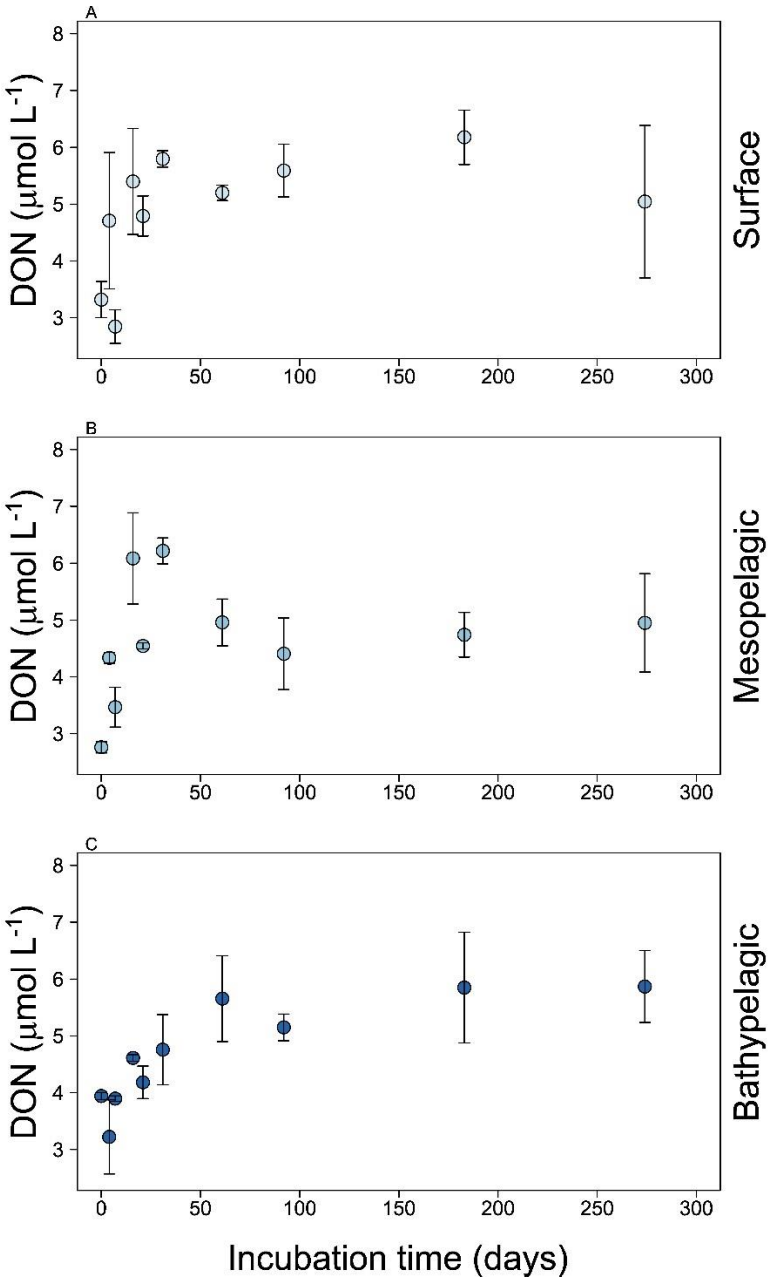

Figure 1. Accumulation of dissolved organic nitrogen over time in experimental bottles using filtered surface water inoculated with surface, mesopelagic or bathypelagic prokaryotic communities in the Labrador Sea. Error bars represent the mean absolute difference between treatment replicates.

Cycling of N-rich DOM pools

Temporal variations in FDOM concentration were monitored to assess the cycling of protein-like ($F_{\lambda em}302$ and $F_{\lambda em}340$) and recalcitrant DOM ($F_{\lambda em}392$), specifically focusing

on N-containing fluorophores. All three components showed noticeable changes over time (Fig. 2). Consistent with DON concentrations, we observed a substantial increase (~3.5 fold) in $F_{\lambda em}302$ in all treatments within the first 31 days of incubation. Subsequently, this fluorophore decreased sharply, returning to levels observed at the start of the incubation by day 92. In deep treatments, there was an overall accumulation until the end of the incubations, not observed in the surface treatment. Peak $F_{\lambda em}340$ fluctuated slightly during the first 92 days, before increasing ~5.5 fold across treatments. Peak $F_{\lambda em}392$ increased linearly over time with R^2 values of 0.79, 0.81 and 0.96 in the bathypelagic, surface, and mesopelagic treatments, respectively (Fig. 2; regressions not shown). This suggests a microbially-mediated release of RDON or a rearrangement of molecules into more recalcitrant forms.

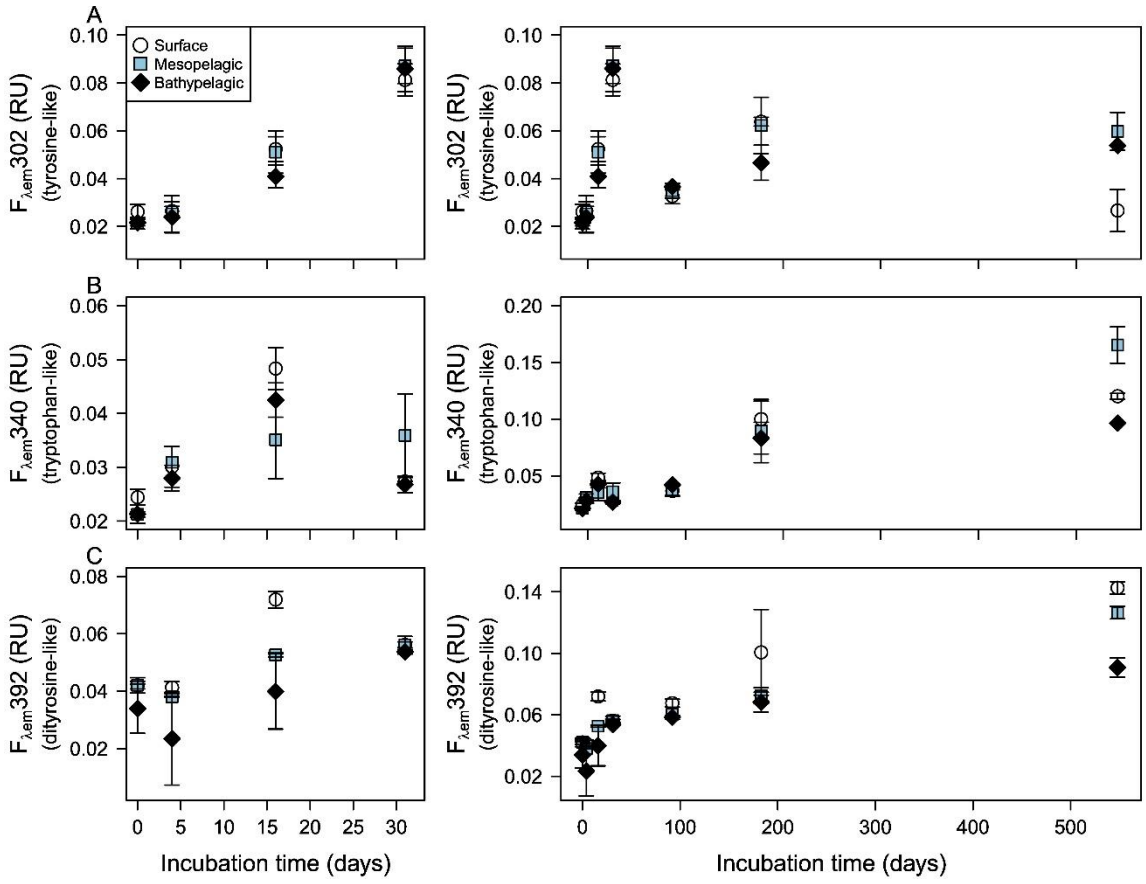

Figure 2. Dynamics of fluorescent N-rich dissolved organic matter pools at different stages of organic matter transformation, and overall accumulation of DON. Peaks $F_{\lambda em}302$ (A) and $F_{\lambda em}340$ (B) are associated with tyrosine and tryptophan, respectively, and are traditionally associated with labile DOM. $F_{\lambda em}392$ (B) has been associated with dityrosine, a molecule recalcitrant to biodegradation. The legend applies for all panels and the error bars represent mean absolute deviations of treatment replicates. The left panels are zoomed on the first 31 days to properly display short-term dynamics and the right panels show the long-term dynamics over the full course of the incubations. Values are reported in Raman units (RU). Note the difference in scale between left and right panels in B and C.

Changes in the relative composition of AA are often used to observe microbial DOM transformations. During the incubation, glycine increased over time whereas L-histidine decreased (Fig. S4), as expected (see SI). In contrast, L-alanine remained relatively stable, and L-serine was highly dynamic. In addition, DI revealed different stages of organic matter transformation. DI increased during the first week, likely because of a *de novo* synthesis of AA during N-immobilization (Fig. 3A, C, E). Then DI values decreased from 1.2-2 to near 0 or negative values in all treatments, indicating significant DON

reprocessing. Similarly, $\%N_{THAA}$ showed decreasing ubiquitous log-linear relationships over time, with R^2 of 0.56, 0.75 and 0.32 in the surface, meso- and bathypelagic treatments, respectively (Fig. 3B, D, F). This suggests the preferential degradation or transformation of AA relative to other DON molecules during the incubation in all water depths.

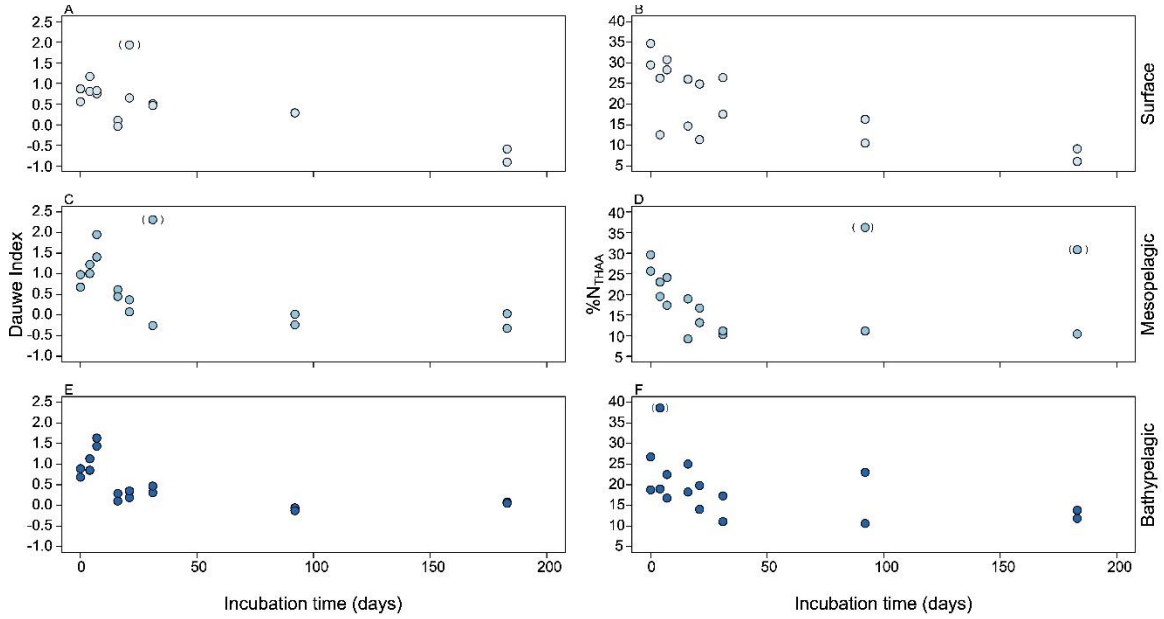

Figure 3. Dynamic cycling of amino acids as shown with the Dauwe Index indicating the production of fresher organic matter in the first stage of incubations followed by microbial reprocessing and progressively more recalcitrant organic matter pool in the surface (A), meso- (C) and bathypelagic treatments (E). Panels B, D and F show the gradual decrease of amino acids nitrogen contribution to the total organic nitrogen pool in the surface, meso- and bathypelagic treatments, respectively. This decrease in $\%N_{THAA}$ is indicative of preferential uptake of amino acids nitrogen over the bulk pool and suggest more degraded organic matter. Points in parentheses were not considered in regressions.

Changes in molecular composition of N-rich DOM

To understand changes in the molecular composition of the DON pool, we characterized a subset of samples using FT-ICR-MS (Fig. 4 and S5). We observed a decrease in the number of assigned N-MF in all compound classes during the incubations (Fig. S5D, E, F), which contrasts with the patterns observed when including all MF (Fig. S5A, B, C, LaBrie et al. 2022). In Van Krevelen diagrams, this was apparent with major losses (dark blue) of N-

MF in low O/C range that spanned most of the H/C range (Fig. 4). All treatments showed some accumulation of N-MF (yellow to dark red). In the surface and mesopelagic treatments, they were situated around O/C ratio of 0.4 and H/C ratio of 1.4 whereas in the bathypelagic, they were of high O/C, low H/C ratios. Overall, the O:C ratio after 92 days of incubation was 0.544±0.019 across treatments, a small but significant increase compared to the initial O:C ratio of 0.523±0.002 (t-test, $p<0.01$). We also observed a high C:N ratio of 221±69 across treatments and over time in the FT-ICR-MS data (not shown), an order of magnitude higher than the DOC:DON ratios (Fig. S3), suggesting a strong bias against nitrogenous molecules of FT-ICR-MS (Podgorski et al. 2012) and SPE-PPL extraction (Jerusalén-Lleó et al. 2023). Nevertheless, these results suggest both a preferential consumption of N-MF over non-N-MF and some production of recalcitrant compounds across treatments.

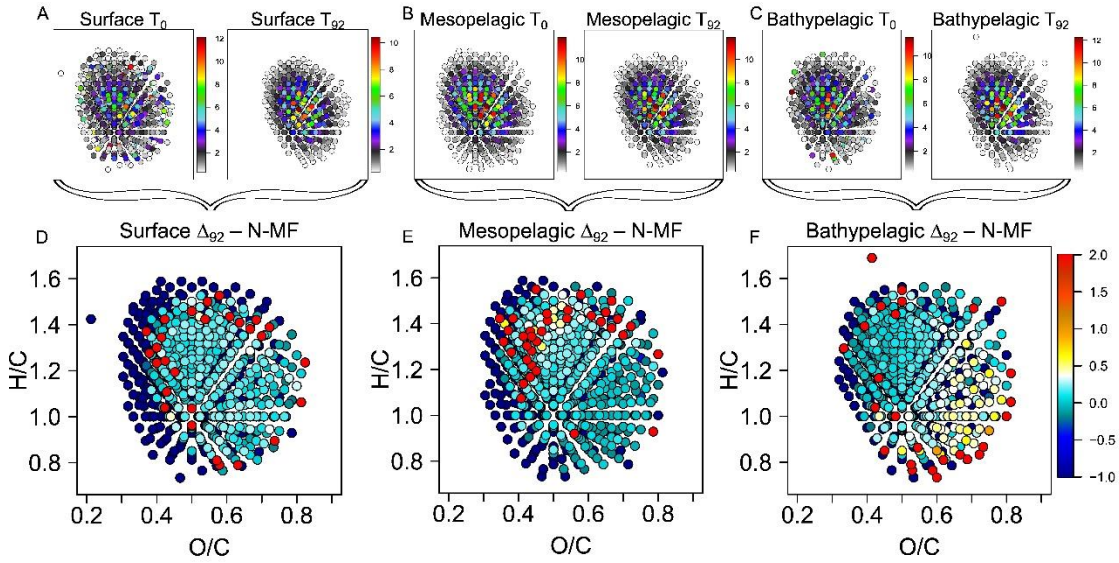

Figure 4. Molecular changes in the surface (A and D), meso- (B and E) and bathypelagic (C and F) treatments showing consumption (blue and dark blue) and production (yellow and red) of N-containing molecular formulas (N-MF).

DISCUSSION

DON production and transformations sequester N

Although labile DON molecules are rapidly consumed in the surface ocean, a substantial proportion of the DON pool resists degradation, even in N limited environments, and accumulates over time (Sipler and Bronk 2015; Zhang et al. 2020). To explain this phenomenon, the MNP suggests that DON reprocessing by microbes leads to the accumulation of stable nitrogenous molecules that resist further degradation (Yamaguchi and McCarthy 2018). Our results support the MNP hypothesis with evidence of microbial production of DON and organic matter reprocessing in surface and deeper depths. DON concentrations reflected an initial rapid build-up that remained relatively stable for the remainder of the incubation. However, FDOM peak $F_{\lambda em}302$ and AA diagenetic indices revealed that this newly synthesized DON was continuously transformed and altered throughout the incubation, in agreement with the turnover time of many centuries for tyrosine-like fluorophores in the deep ocean (Catalá et al. 2015). Thus, prokaryotic communities from all oceanic depths harbor the metabolic potential to produce long-lived DON.

Potential chemical structure of refractory DON

Chemical recalcitrance is thought to be a major factor in RDOM sequestration, for both C and N (Jiao et al. 2010; Broek et al. 2023). With regards to RDOC, carboxyl-rich alicyclic molecules (CRAM) and other oxygen-rich molecules are thought to be classes of compounds that are intrinsically resistant to microbial degradation (Hertkorn et al. 2006;

LaBrie et al. 2022). For RDON, we did observe an increase in O:C ratio in N-MF over time. However, this increase was likely related to a higher consumption of low O:C over high O:C molecules as all classes of MF were consumed over time (Fig. S5). This suggests a fundamental difference between DOC and DON sequestration as high O:C molecules production was observed in the MCP (LaBrie et al. 2022). Potential candidates for the RDON pool are N-heterocycles, aromatic rings composed with at least one N atom. N-heterocycles were found to dominate NMR spectra in the LMW fraction of all oceanic depths (Broek et al. 2023). No sign of their enrichment, as unsaturated compounds, was detected here with FT-ICR-MS, but this technique appears biased against N-molecules (Podgorski et al. 2012; Jerusalén-Lleó et al. 2023). Using fluorescence spectroscopy, we found a potential source for one of these N-heterocycles in all treatments, the indole structure that gives its fluorescence property to tryptophan (peak $F_{\lambda em}340$). While this fluorophore has been associated with bioavailable DOM in the surface ocean (Lønborg et al. 2010), there are other studies showing its accumulation in prokaryotic biodegradation experiments (Moran et al. 2000). This differential behavior in tryptophan-like cycling could be explained by its origin. Higher emission wavelength maximum (e.g., Lønborg et al. 2010) is produced by phytoplankton and likely protein-bounded (Romera-Castillo et al. 2010) whereas lower emission maximum is associated with prokaryotic production (Lakowicz 1983) and may represent pure tryptophan (Yamashita and Tanoue 2003) or pure indole (Ménez et al. 2018).

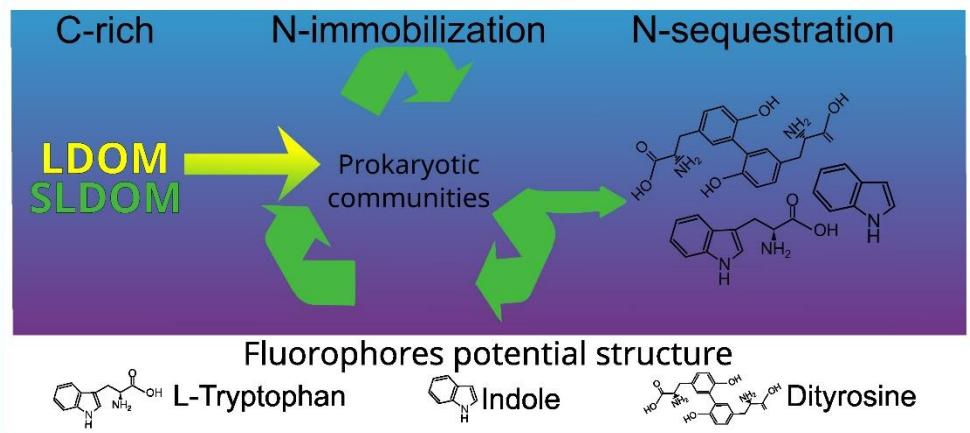

Figure 5. Conceptual diagram representing the microbial nitrogen pump in our experiment. Carbon-rich labile and semilabile molecules (e.g. polysaccharides, exopolymers) are taken up by microorganisms and reprocessed, immobilizing nitrogen in the process. A small proportion of the dissolved organic matter becomes refractory, sequestering nitrogen.

RDON production likely dominant in the surface ocean

The production of RDON, and refractory DOM in general, requires the combination of two key components: the metabolic pathways of the microbial community to produce stable compounds and bioavailable substrate that can be reprocessed. We found that prokaryotic communities from all depths were adapted to produce RDON from similar starting substrates (Fig. S1). As such, substrate bioavailability most probably impacts RDON production rate. Except for rare regions where relatively fresh surface DOM can be deeply entrained (Tian et al. 2004), the deep ocean is severely substrate limited, whereas the surface ocean DOM pool is continuously replenished with fresh DOM exuded by primary producers (Nagata 2000). This supports an independent assessment of the MNP using N stable isotopes where it was hypothesized that the majority of RDON production occurred in the surface ocean from a direct production of intrinsically stable molecules (Ianiri and McCarthy 2023). Given that little RDON was produced in the early stages of incubations when more labile DOM was available, we hypothesize that prokaryotic communities also

transform a fraction of the semi-labile pool into more refractory molecules (Fig. 5), constraining RDON production predominantly to the top few hundred meters of the ocean.

CONCLUSION

We show the production of N-rich compounds that persisted for several months across water depths inoculated with different prokaryotic communities in bottle experiments. The accumulated N was not simply stored, but showed multiple signs of reprocessing, including changes in fluorescent properties and AA composition. Overall, our results have important implications on global DOM cycling, particularly if we consider that bioavailable DOM supply limits RDON production. DOM in our experiments was apparently rich in polysaccharides and RDON production likely started once that pool of labile DOM was exhausted. As many blooming phytoplankton taxa produce these transparent exopolymers (Passow 2002), blooms may not only be hot moments of high CO_2 drawdown, but also in DON production resulting in combined long term N and C sequestration.

Acknowledgements

We'd like to thank the crew members of the *CCGS Hudson* and chief scientist during the cruise Igor Yashayaev. This work was supported by a NSERC—Climate Change and Atmospheric Research (CCAR) to the Ventilation, Interactions and Transports Across the Labrador Sea (VITALS) program to RM, a NSERC Discovery grants to RM and LT as well as UdeM and FRQNT student scholarships, and McGill Wares and Trottier Space Institute postdoctoral fellowship to RL.

Data and code availability

All scripts and data that were originally published by LaBrie et al. (2022) are available at http://www.github.com/LaboMaranger/MCP and the new data and scripts are available at http://www.github.com/LaboMaranger/MNP.

References

Aluwihare, L. I., and T. Meador. 2008. Chapter 3 - Chemical Composition of Marine Dissolved Organic Nitrogen, p. 95–140. *In* D.G. Capone, D.A. Bronk, M.R. Mulholland, and E.J. Carpenter [eds.], Nitrogen in the Marine Environment (Second Edition). Academic Press.

Amon, R. M. W., H. P. Fitznar, and R. Benner. 2001. Linkages among the bioreactivity, chemical composition, and diagenetic state of marine dissolved organic matter. Limnol. Oceanogr. **46**: 287–297. doi:10.4319/lo.2001.46.2.0287

Benner, R., and R. M. Amon. 2015. The size-reactivity continuum of major bioelements in the ocean. Annu. Rev. Mar. Sci. **7**: 185–205. doi:10.1146/annurev-marine-010213-135126

Benner, R., and B. Biddanda. 1998. Photochemical transformations of surface and deep marine dissolved organic matter: Effects on bacterial growth. Limnol. Oceanogr. **43**: 1373–1378. doi:10.4319/lo.1998.43.6.1373

Bourgoin, L.-H., and L. Tremblay. 2010. Bacterial reworking of terrigenous and marine organic matter in estuarine water columns and sediments. Geochim. Cosmochim. Acta **74**: 5593–5609. doi:10.1016/j.gca.2010.06.037

394 Broek, T. A. B., A. L. Bour, H. L. Ianiri, T. P. Guilderson, and M. D. McCarthy. 2019.
395 Amino acid enantiomers in old and young dissolved organic matter: Implications
396 for a microbial nitrogen pump. Geochim. Cosmochim. Acta **247**: 207–219.
397 doi:10.1016/j.gca.2018.12.037
398 Broek, T. A. B., M. D. McCarthy, H. L. Ianiri, J. S. Vaughn, H. E. Mason, and A. N. Knapp.
399 2023. Dominant heterocyclic composition of dissolved organic nitrogen in the
400 ocean: A new paradigm for cycling and persistence. Proc. Natl. Acad. Sci. **120**:
401 e2305763120. doi:10.1073/pnas.2305763120
402 Catalá, T. S., I. Reche, A. Fuentes-Lema, and others. 2015. Turnover time of fluorescent
403 dissolved organic matter in the dark global ocean. Nat. Commun. **6**.
404 doi:10.1038/ncomms6986
405 Coble, P. G. 1996. Characterization of marine and terrestrial DOM in seawater using
406 excitation-emission matrix spectroscopy. Mar. Chem. **51**: 325–346.
407 doi:10.1016/0304-4203(95)00062-3
408 Cowie, G. L., and J. I. Hedges. 1994. Biochemical indicators of diagenetic alteration in
409 natural organic matter mixtures. Nature **369**: 304–307. doi:10.1038/369304a0
410 Dauwe, B., J. J. Middelburg, P. M. Herman, and C. H. Heip. 1999. Linking diagenetic
411 alteration of amino acids and bulk organic matter reactivity. Limnol. Oceanogr. **44**:
412 1809–1814. doi:10.4319/lo.1999.44.7.1809
413 Davis, J., K. Kaiser, and R. Benner. 2009. Amino acid and amino sugar yields and
414 compositions as indicators of dissolved organic matter diagenesis. Org. Geochem.
415 **40**: 343–352. doi:10.1016/j.orggeochem.2008.12.003

Dittmar, T., B. Koch, N. Hertkorn, and G. Kattner. 2008. A simple and efficient method for the solid-phase extraction of dissolved organic matter (SPE-DOM) from seawater. Limnol. Oceanogr. Methods **6**: 230–235. doi:10.4319/lom.2008.6.230

Escoubeyrou, K., and L. Tremblay. 2014. Quantification of free, dissolved combined, particulate, and total amino acid enantiomers using simple sample preparation and more robust chromatographic procedures. Limnol. Oceanogr.-Methods **12**: 421–431. doi:10.4319/lom.2014.12.421

Hansell, D. A. 2005. Dissolved Organic Carbon Reference Material Program. Eos Trans. Am. Geophys. Union **86**: 318–318. doi:10.1029/2005EO350003

Hawkes, J. A., J. D'Andrilli, J. N. Agar, and others. 2020. An international laboratory comparison of dissolved organic matter composition by high resolution mass spectrometry: Are we getting the same answer? Limnol. Oceanogr. Methods **18**: 235–258. doi:https://doi.org/10.1002/lom3.10364

Hébert, M., and L. Tremblay. 2017. Production and persistence of bacterial and labile organic matter at the hypoxic water–sediment interface of the St. Lawrence Estuary. Limnol. Oceanogr. **62**: 2154–2167. doi:10.1002/lno.10556

Hertkorn, N., R. Benner, M. Frommberger, P. Schmitt-Kopplin, M. Witt, K. Kaiser, A. Kettrup, and J. I. Hedges. 2006. Characterization of a major refractory component of marine dissolved organic matter. Geochim. Cosmochim. Acta **70**: 2990–3010. doi:10.1016/j.gca.2006.03.021

Holmes, R. M., A. Aminot, R. Kérouel, B. A. Hooker, and B. J. Peterson. 1999. A simple and precise method for measuring ammonium in marine and freshwater ecosystems. Can. J. Fish. Aquat. Sci. **56**: 1801–1808.

Ianiri, H. L., and M. D. McCarthy. 2023. Compound specific δ15N analysis of amino acids reveals unique sources and differential cycling of high and low molecular weight marine dissolved organic nitrogen. Geochim. Cosmochim. Acta **344**: 24–39. doi:10.1016/j.gca.2023.01.008

Jerusalén-Lleó, E., M. Nieto-Cid, I. Fuentes-Santos, T. Dittmar, and X. A. Álvarez-Salgado. 2023. Solid phase extraction of ocean dissolved organic matter with PPL cartridges: efficiency and selectivity. Front. Mar. Sci. **10**. doi:10.3389/fmars.2023.1159762

Jiao, N., G. J. Herndl, D. A. Hansell, and others. 2010. Microbial production of recalcitrant dissolved organic matter: long-term carbon storage in the global ocean. Nat. Rev. Microbiol. **8**: 593–599. doi:10.1038/nrmicro2386

LaBrie, R., S. Bélanger, R. Benner, and R. Maranger. 2020. Spatial abundance distribution of prokaryotes is associated with dissolved organic matter composition and ecosystem function. Limnol. Oceanogr. **66**: 575–587. doi:10.1002/lno.11624

LaBrie, R., B. Péquin, N. Fortin St-Gelais, and others. 2022. Deep ocean microbial communities produce more stable dissolved organic matter through the succession of rare prokaryotes. Sci. Adv. **8**: eabn0035. doi:10.1126/sciadv.abn0035

Lakowicz, J. R. 1983. Principles of Fluorescence Spectroscopy, Plenum Press.

Larsson, M. E., A. R. Bramucci, S. Collins, G. Hallegraeff, T. Kahlke, J.-B. Raina, J. R. Seymour, and M. A. Doblin. 2022. Mucospheres produced by a mixotrophic protist impact ocean carbon cycling. Nat. Commun. **13**: 1301. doi:10.1038/s41467-022-28867-8

461 Lechtenfeld, O. J., G. Kattner, R. Flerus, S. L. McCallister, P. Schmitt-Kopplin, and B. P.
462 Koch. 2014. Molecular transformation and degradation of refractory dissolved
463 organic matter in the Atlantic and Southern Ocean. Geochim. Cosmochim. Acta
464 **126**: 321–337. doi:10.1016/j.gca.2013.11.009
465 Lønborg, C., and X. A. Álvarez-Salgado. 2012. Recycling versus export of bioavailable
466 dissolved organic matter in the coastal ocean and efficiency of the continental shelf
467 pump. Glob. Biogeochem. Cycles **26**. doi:10.1029/2012GB004353
468 Lønborg, C., X. A. Álvarez-Salgado, K. Davidson, S. Martínez-García, and E. Teira. 2010.
469 Assessing the microbial bioavailability and degradation rate constants of dissolved
470 organic matter by fluorescence spectroscopy in the coastal upwelling system of the
471 Ría de Vigo. Mar. Chem. **119**: 121–129. doi:10.1016/j.marchem.2010.02.001
472 McCarthy, M., T. Pratum, J. Hedges, and R. Benner. 1997. Chemical composition of
473 dissolved organic nitrogen in the ocean. Nature **390**: 150–154. doi:10.1038/36535
474 Ménez, B., C. Pisapia, M. Andreani, and others. 2018. Abiotic synthesis of amino acids in
475 the recesses of the oceanic lithosphere. Nature **564**: 59–63. doi:10.1038/s41586-
476 018-0684-z
477 Moran, M. A., W. M. Sheldon Jr., and R. G. Zepp. 2000. Carbon loss and optical property
478 changes during long-term photochemical and biological degradation of estuarine
479 dissolved organic matter. Limnol. Oceanogr. **45**: 1254–1264.
480 doi:10.4319/lo.2000.45.6.1254
481 Murphy, K. R., C. A. Stedmon, P. Wenig, and R. Bro. 2014. OpenFluor- an online spectral
482 library of auto-fluorescence by organic compounds in the environment. Anal.
483 Methods **6**: 658–661. doi:10.1039/C3AY41935E

Nagata, T. 2000. Production mechanisms of dissolved organic matter, p. 121–152. *In* D.L. Kirchman [ed.], Microbial ecology of the oceans. Wiley Series in Ecological and Applied Microbiology.

Ogawa, H., Y. Amagai, I. Koike, K. Kaiser, and R. Benner. 2001. Production of Refractory Dissolved Organic Matter by Bacteria. Science **292**: 917–920. doi:10.1126/science.1057627

Paerl, R. W., I. M. Claudio, M. R. Shields, T. S. Bianchi, and C. L. Osburn. 2020. Dityrosine formation via reactive oxygen consumption yields increasingly recalcitrant humic-like fluorescent organic matter in the ocean. Limnol. Oceanogr. Lett. **5**: 337–345. doi:10.1002/lol2.10154

Passow, U. 2002. Transparent exopolymer particles (TEP) in aquatic environments. Prog. Oceanogr. **55**: 287–333. doi:10.1016/S0079-6611(02)00138-6

Péquin, B., R. LaBrie, N. F. St-Gelais, and R. Maranger. 2022. Succession of protistan functional traits is influenced by bloom timing. Front. Mar. Sci. **9**. doi:10.3389/fmars.2022.916093

Podgorski, D. C., A. M. McKenna, R. P. Rodgers, A. G. Marshall, and W. T. Cooper. 2012. Selective ionization of dissolved organic nitrogen by positive ion atmospheric pressure photoionization coupled with Fourier transform ion cyclotron resonance mass spectrometry. Anal. Chem. **84**: 5085–5090. doi:10.1021/ac300800w

R Core Team. 2022. R: A Language and Environment for Statistical Computing, R Foundation for Statistical Computing.

505 Romera-Castillo, C., H. Sarmento, X. A. Alvarez-Salgado, J. M. Gasol, and C. Marrase.
506 2010. Production of chromophoric dissolved organic matter by marine
507 phytoplankton. Limnol. Oceanogr. **55**: 446–454. doi:10.4319/lo.2010.55.1.0446
508 Romera-Castillo, C., H. Sarmento, X. A. Álvarez-Salgado, J. M. Gasol, and C. Marrasé.
509 2011. Net Production and Consumption of Fluorescent Colored Dissolved Organic
510 Matter by Natural Bacterial Assemblages Growing on Marine Phytoplankton
511 Exudates. Appl. Environ. Microbiol. **77**: 7490–7498. doi:10.1128/AEM.00200-11
512 Sipler, R. E., and D. A. Bronk. 2015. Dynamics of Dissolved Organic Nitrogen, p. 127–
513 232. *In* D.A. Hansell and C.A. Carlson [eds.], Biogeochemistry of Marine
514 Dissolved Organic Matter. Academic Press.
515 Tian, R. C., D. Deibel, R. B. Rivkin, and A. F. Vézina. 2004. Biogenic carbon and nitrogen
516 export in a deep-convection region: simulations in the Labrador Sea. Deep Sea Res.
517 Part Oceanogr. Res. Pap. **51**: 413–437. doi:10.1016/j.dsr.2003.10.015
518 Tillmann, U., A. Mitra, K. J. Flynn, and M. E. Larsson. 2023. Mucus-Trap-Assisted
519 Feeding Is a Common Strategy of the Small Mixoplanktonic Prorocentrum
520 pervagatum and P. cordatum (Prorocentrales, Dinophyceae). Microorganisms **11**:
521 1730. doi:10.3390/microorganisms11071730
522 Tremblay, L., and R. Benner. 2006. Microbial contributions to N-immobilization and
523 organic matter preservation in decaying plant detritus. Geochim. Cosmochim. Acta
524 **70**: 133–146. doi:10.1016/j.gca.2005.08.024
525 Tremblay, L., and R. Benner. 2009. Organic matter diagenesis and bacterial contributions
526 to detrital carbon and nitrogen in the Amazon River system. Limnol. Oceanogr. **54**:
527 681–691. doi:10.4319/lo.2009.54.3.0681

Yamaguchi, Y. T., and M. D. McCarthy. 2018. Sources and transformation of dissolved and particulate organic nitrogen in the North Pacific Subtropical Gyre indicated by compound-specific δ15N analysis of amino acids. Geochim. Cosmochim. Acta **220**: 329–347. doi:10.1016/j.gca.2017.07.036

Yamashita, Y., Y. Mori, and H. Ogawa. 2023. Hydrothermal-derived black carbon as a source of recalcitrant dissolved organic carbon in the ocean. Sci. Adv. **9**: eade3807. doi:10.1126/sciadv.ade3807

Yamashita, Y., and E. Tanoue. 2003. Chemical characterization of protein-like fluorophores in DOM in relation to aromatic amino acids. Mar. Chem. **82**: 255–271. doi:10.1016/S0304-4203(03)00073-2

Yashayaev, I., and J. W. Loder. 2017. Further intensification of deep convection in the Labrador Sea in 2016. Geophys. Res. Lett. **44**: 1429–1438. doi:10.1002/2016GL071668

Zhang, X., B. B. Ward, and D. M. Sigman. 2020. Global Nitrogen Cycle: Critical Enzymes, Organisms, and Processes for Nitrogen Budgets and Dynamics. Chem. Rev. **120**: 5308–5351. doi:10.1021/acs.chemrev.9b00613